

Synthesis, crystal structure and Hirshfeld surface analysis of *tert*-butyl *N*-acetylcarbamateAly Dawa El Mestehdi,^a Moctar Abba,^b Mohamed Lemine El Housseine,^c Abderrahmane Ould Hadou,^a Aliou Hamady Barry,^a Brahim Ould Elemine,^a Christian Jelsch^d and Mohamed Gaye^{e*}Received 31 March 2022
Accepted 26 September 2022

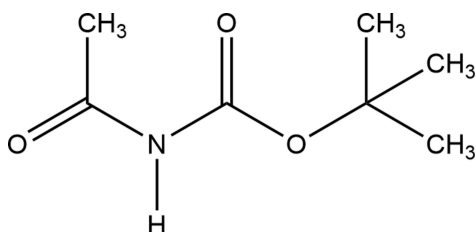
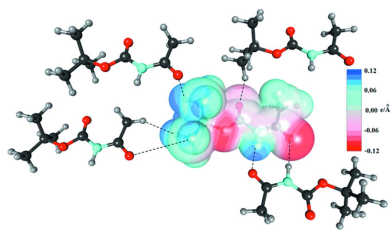
Edited by A. S. Batsanov, University of Durham, England

Keywords: X-ray crystal structure; *tert*-butyl acetylcarbamate; natural phosphate; Mauritanian phosphate deposit.**CCDC reference:** 2209649**Supporting information:** this article has supporting information at journals.iucr.org/e^aUnité de Chimie Moléculaire et Environnement, Département de Chimie, FST, UNA, Nouakchott, Mauritania, ^bDépartement des Sciences Exactes, Ecole Normale Supérieure de Nouakchott, Nouakchott, Mauritania, ^cAgence Nationale de Recherches Géologiques et du Patrimoine Minier (ANARPAM), Nouakchott, Mauritania, ^dLaboratoire CRM², CNRS, Institut Jean Barriol, Université de Lorraine, 54000, Nancy, France, and ^eDépartement de Chimie, Faculté des Sciences et Techniques, Université Cheik Anta Diop, Dakar, Senegal. *Correspondence e-mail: mlgayeastou@yahoo.fr

This article reports a practical synthesis of *tert*-butyl acetylcarbamate, C₇H₁₃NO₃, from *N*-Boc-thioacetamide and the study of its crystal structure. The reaction proceeds in the presence of natural phosphate as a catalyst, with excellent yield, simple workup and benign environment. The crystal structure was refined using a transferred multipolar atom model. In the crystal, symmetrical pairs of strong N—H···O hydrogen bonds connect the molecules into dimers with an R₂²(8) ring motif. The interactions between neighbouring dimers are mostly van der Waals, between hydrophobic methyl groups. Hirshfeld surface analysis shows the major contributions to the crystal packing are from H···H (42.6%) and O···H (26.7%) contacts.

1. Chemical context

Carbamates are widely used as agrochemicals, in the polymer industry, in peptide synthesis (Dibenedetto *et al.*, 2002) and in medicinal chemistry, where many derivatives are specifically designed to make drug–target interactions through their carbamate moiety (Ghosh & Brindisi, 2015). Here we report the crystal structure of *tert*-butyl-acetylcarbamate, C₇H₁₃NO₃ (I), which we obtained while attempting to synthesize poly-functional amidines (which are useful in synthetic fields, especially as templates for the development of various novel heterocycles) using heterogeneous catalysis on natural phosphates (NP) – readily available, stable, easy to handle and regenerate, non-toxic and inexpensive catalysts with both basic and acidic active sites (Sebti *et al.*, 1994, 1996).



We followed the procedure described by Lee *et al.* (1998), but using natural phosphate (NP) as a catalyst instead of Lewis acids such as ZnCl₂, Et₃O⁺BF₄⁻ and FeCl₂. The synthesis was carried out by blending *N*-(*t*-Boc)thioacetamide with various aminoesters, in the presence of NEt₃ and NP. The

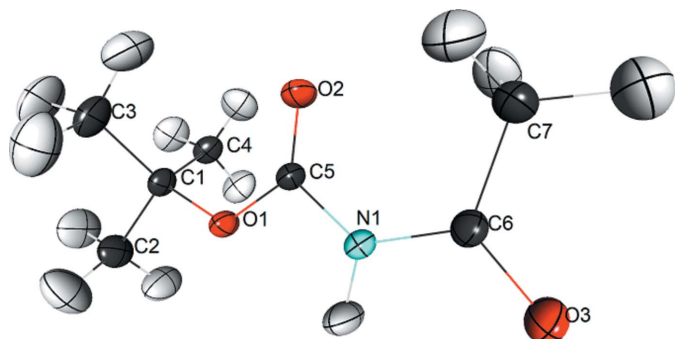


Figure 1
View of molecule (I), showing the atom-labelling scheme. Displacement ellipsoids are drawn at the 50% probability level.

reaction yielded (I) instead of the desired amidine, *i.e.* the sulfur atom was substituted by oxygen. In the absence of NP, no product was obtained and the starting materials were recovered.

2. Structural commentary

The title compound, $C_7H_{13}NO_3$, (Fig. 1) crystallizes in the space group $P2_1/n$ with one molecule per asymmetric unit. The

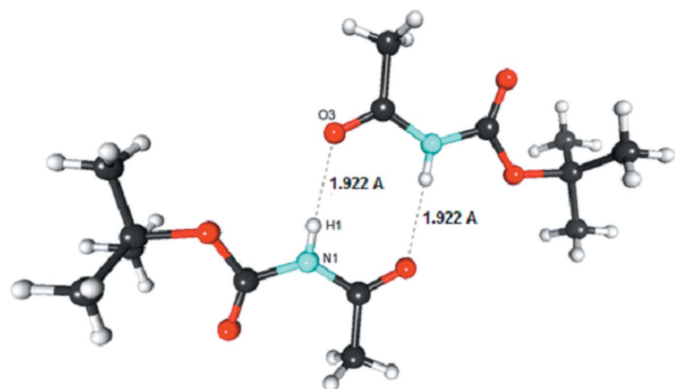


Figure 2
View of the molecular dimer linked by a double hydrogen bond.

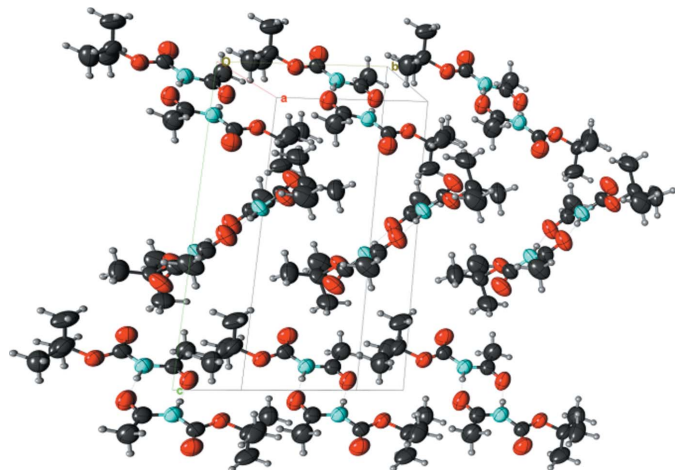


Figure 3
Molecular packing of (I), viewed along the a axis, showing different orientations of the dimers.

Table 1
Hydrogen-bond geometry (\AA , $^\circ$).

$D-H\cdots A$	$D-H$	$H\cdots A$	$D\cdots A$	$D-H\cdots A$
$C4-H4A\cdots O2$	1.10	2.48	3.0651 (14)	112
$C3-H3C\cdots O2$	1.10	2.49	2.9928 (15)	107
$N1-H1\cdots O3^i$	1.01 (1)	1.92 (1)	2.9285 (11)	173 (1)

Symmetry code: (i) $-x + 1, -y, -z + 1$.

skeleton of the molecule is nearly planar if the C3 and C4 atoms are excluded, the root-mean-square deviation from the mean plane being 0.070 \AA . The $C3H_3$ and $C4H_3$ methyl groups, located on either side of the mean plane, generate two weak intramolecular hydrogen bonds with the carbonyl O2 atom located in the plane [$C3-H3C\cdots O2$ and $C4-H4A\cdots O2$, $d(H\cdots O) = 2.49$ and 2.48 \AA , respectively; Table 1].

3. Supramolecular features

In the crystal, a centrosymmetric dimer of molecules is held together by two $N-H\cdots O=C$ hydrogen bonds, $N1-H1\cdots O3$ and its symmetry equivalent [$d(H\cdots O) = 1.92$ (1) \AA , Table 1], which represent the strongest interactions in the packing and create an inversion-symmetric supramolecular motif of graph-set $R_2^2(8)$ (Fig. 2). Fig. 3 shows the packing of these dimers. If we consider the Hirshfeld surface around the dimer *as a whole*, this surface is constituted mainly by hydrophobic (C and H-c) atoms (81%) and oxygen atoms (13%). The interactions between neighbouring dimers are mostly hydrophobic: $H-c\cdots H-c$ between methyl groups (43%) and $C\cdots H-c$ between carbonyl and methyl groups (21%). Weak $C-H\cdots O$ hydrogen bonds also occur between dimers (23%). The steric hindrance of the methyl groups causes an offset of the molecules of consecutive dimers, so that no strong hydrogen bond is observed between the dimers. Consequently, the crystal appears to be stabilized by strong hydrogen bonding within the dimers and van der Waals forces without.

4. Hirshfeld analysis

MoProViewer (Jelsch *et al.*, 2005) was used to further investigate and visualize the intermolecular interactions in the crystal. The Hirshfeld surface was computed from the model

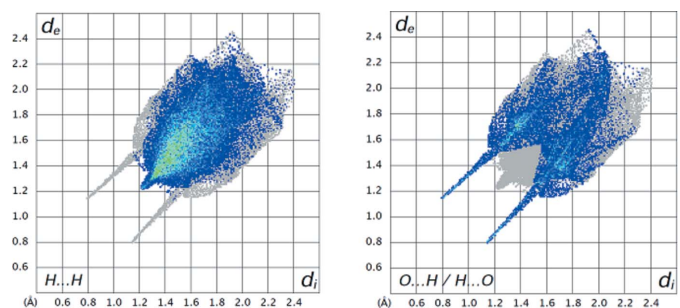


Figure 4
Two-dimensional fingerprint plots of the major contacts on the Hirshfeld surface.

Table 2

Statistical analysis of intermolecular contacts on the Hirshfeld surface.

 H-c and H-n signify hydrogen atoms bound to C (hydrophobic) and N (hydrophilic), respectively. Reciprocal contacts ($X\cdots Y$ and $Y\cdots X$) are merged. The most prevalent and enriched contacts are highlighted in bold.

Atom	H-n	N	O	H-c	C
S_x (%)	5.5	1.5	15.5	64.0	13.5
C_{xy} (%) (E_{xy})					
H-n	0.4 (1.39)				
N	0 (0)	0 (0)			
O	5.9 (3.41)	0 (0)	0.4 (0.16)		
H-c	4.2 (0.59)	2.8 (1.46)	20.8 (1.04)	41.6 (0.99)	
C	0.2 (0.13)	0.1 (0.41)	3.4 (0.86)	18.5 (1.12)	1.6 (1.00)

after multipolar refinement but using electron density from the spherical-neutral atom model. The 2D fingerprint plots (Fig. 4) were generated with *Crystal Explorer* (Spackman *et al.*, 2021). The most significant contributions for the contacts in the crystal packing (Table 2) are from H \cdots H (46.2%), O \cdots H/H \cdots O (26.7%) and C \cdots H/H \cdots C contacts (18.7%), whereas only 2.8% are from N \cdots H/H \cdots N contacts. In the fingerprint plots (Fig. 4), the two reciprocal spikes at a short distance correspond to the O \cdots H–N/N–H \cdots O contacts, *i.e.* strong hydrogen bonds. The H \cdots H contacts show also a small spike on the diagonal line, the shortest distances being 2.447 Å between H2B and H7A($x + 1, y - 1, z$) (Fig. 5a). The intermolecular interactions were further evaluated by computing

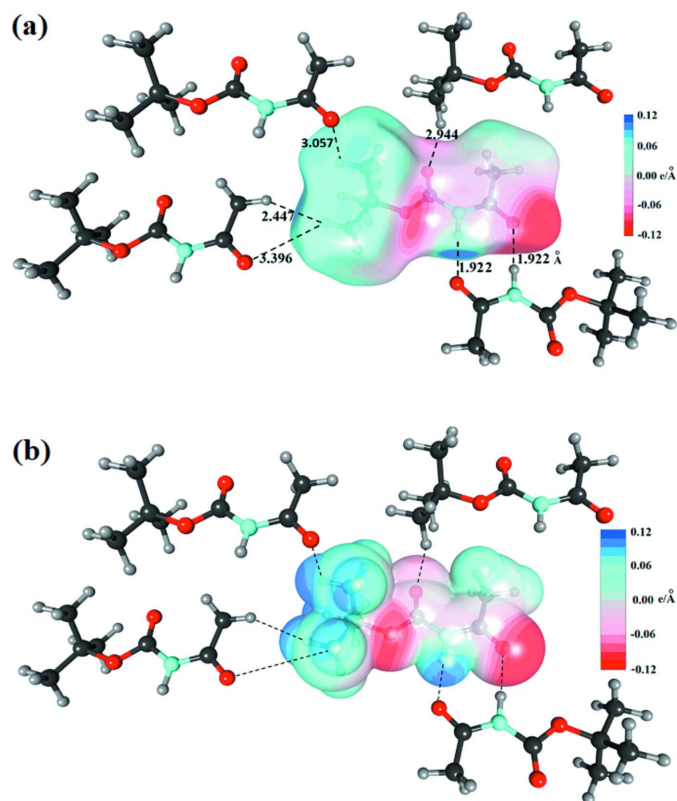


Figure 5

(a) Hirshfeld and (b) van der Waals surfaces around molecule (I). The N–H \cdots O and C–H \cdots O hydrogen bonds as well as a short H \cdots H contacts are shown. The surfaces are coloured according to the electrostatic potential.

the enrichment ratios (E , see Table 2) in order to highlight which contacts are over-represented and are likely to represent energetically strong interactions and be the driving force in crystal formation (Jelsch *et al.*, 2014). The enrichment values are obtained as the ratio between the shares of actual contacts C_{xy} and the random (equiprobable) contacts R_{xy} , the latter calculated as if all types of contacts had the same propensity to occur and are obtained by probability products ($R_{xy} = S_x \cdot S_y$). The H-c \cdots H-c hydrophobic contacts are the most abundant on the Hirshfeld surface but have a unitary enrichment ratio. The O \cdots H-c and C \cdots H-c weak hydrogen bonds are the next most abundant interactions and are slightly enriched ($E = 1.04$ and 1.12, respectively). While the strong O \cdots H-n hydrogen bonds in the fourth position represent only 5.9% of the contact surface, they are the most enriched at $E = 3.41$. The H-c \cdots N contacts are over-represented with $E = 1.46$ as the nitrogen atom interacts mostly with methyl groups on both sides of the sp^2 plane.

The Hirshfeld surface was partitioned into (H-c, C) and (H-n, O, N) atoms' shares in order to analyse the contacts in terms of hydrophobic and hydrophilic interactions. Overall, hydrophobic atoms (C and H-c) comprise 77.5% of the surface, but the hydrophobic contacts between these atoms (61.8%) are not significantly enriched at $E = 1.03$. Contacts between hydrophilic atoms (22.5% of the surface), mostly in the form of strong hydrogen bonds, are enriched to 6.7% ($E = 1.32$) while cross-interactions (between hydrophobic and hydrophilic atoms) are under-represented (31.6%, $E = 0.90$).

The electrostatic potential was computed on the Hirshfeld and van der Waals surfaces of the molecule (Fig. 5). The two surfaces show similar potential values which are both in the -0.12 to $+0.12$ e Å $^{-1}$ range. The regions around the three oxygen atoms are electronegative while the NH group displays positive potential on the surface, followed by the methyl groups which are moderately electropositive.

5. Database survey

The Cambridge Structural Database (Version 5.43, November 2021; Groom *et al.*, 2016) was surveyed using *ConQuest* (version 2020.2.0; Bruno *et al.*, 2002). The eight-membered supramolecular motif, with a double N–H \cdots O=C hydrogen bond between two amide groups, is quite common, being encountered in 10,336 crystal structures. The amide-ester fragment, encountered in 35 structures, exists in three different near-planar conformations (Fig. 6). Conformation (a) with the *syn* disposition of C=O bonds appears in 23 structures, including the nearest reported analogue of (I),

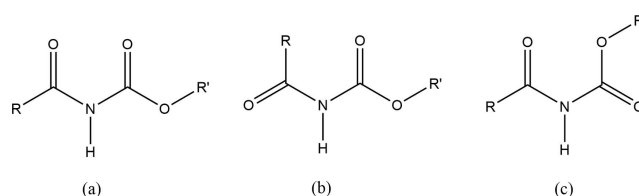


Figure 6

Conformations of amide-ester derivatives.

Table 3

X-ray fluorescence (XRF) analysis (%) of natural phosphate.

SiO ₂	TiO ₂	Al ₂ O ₃	Fe ₂ O ₃	MgO	CaO	Na ₂ O	K ₂ O	MnO	P ₂ O ₅	SO ₃
14.17	0.058	17.51	0.530	0.245	31.66	0.319	0.113	0.016	26.18	0.060

1,1-dimethylethyl-*N*-propanoylcarbamate (II) (Brodesser *et al.*, 2003). Two different *anti* conformations, (*b*) and (*c*), are adopted by nine and three compounds, respectively. Molecule (I) adopts the *anti* conformation (*b*). Compound (I) is the homologue of (II).

6. Synthesis and crystallization

Materials and physical methods. All reagents were purchased from Sigma-Aldrich. Reaction progress was monitored by thin-layer chromatography (TLC) on silica-gel plates (Fluka Kieselgel 60 F254). Flash chromatography purifications were performed on Interchim Puriflash (Puriflash columns 50 μ). X-ray fluorescence analysis was performed on a PANalytical AxiosmAX spectrometer.

Preparation of the catalyst. The NP used in this work comes from the Bofal phosphate deposit in Mauritania. Before being used in catalysis, it underwent quartering treatment, particle-size separation, aqueous dissolution, filtration and evaporation of water, calcination at 1173 K for 1 h and grinding. The fraction of 60–100 μ m grain size was used. The nominal chemical compositions of this phosphate were given by X-ray fluorescence (XRF) analysis. The total amount of the natural inorganic components was 90.86% (Table 3). The rest was mainly organic matter, as indicated by the weight loss on combustion, which amounted to 10.43%.

Preparation of tert-butyl acetylcarbamate (I). It should be noted that compound (I) was prepared in our attempt to synthesize polyfunctional amidines, which are useful in synthetic fields, especially as a template for the development of various new heterocycles. In the preparation, we used the same operating conditions as Lee *et al.* (1998), substituting NP as the catalyst for a Lewis acid. To a solution of *N*-(*t*-Boc)thioacetamide (87.6 mg; 0.5 mmol), the hydrochloride salt of an amino ester (0.5 mmol) and triethylamine (1.65 mmol) in a dry solvent (10 mL), NP (87.6 mg) was added with stirring. The reaction was stirred for 30 min at room temperature. The mixture was filtered through a pad of celite. The residue was purified by Interchim Puriflash (Puriflash columns 50 μ) using a cyclohexane/ethyl acetate eluent system, to yield crystalline (I) in a very high yield ($\geq 95\%$). We have tested this reaction with various solvents (THF, CH₃CN and DMF) and hydrochlorides of different amino esters, *viz.* glycine ethyl ester, L-valine methyl ester, L-alanine ethyl ester and L-phenylalanine methyl ester. *N*-(Boc)thioacetamide was prepared as described in the literature (Lee *et al.*, 1998).

7. Refinement

Crystal data, data collection and structure refinement details are summarized in Table 4. A least-squares refinement, based

on $|F|^2$ of all reflections, was carried out with the program *MoPro* (Jelsch *et al.*, 2005) using the *ELMAM2* electron-density database (Domagała *et al.*, 2012). In this approach, scale factors, atomic positions and displacement parameters for all atoms were varied, but a multipolar charged-atom model was applied until convergence. The H–X distances were constrained to the standard values in neutron diffraction studies (Allen & Bruno, 2010). The anisotropic displacement parameters of hydrogen atoms were constrained to the values obtained from the *SHADE3* server (Madsen & Hoser, 2014). Two subsets of the molecule (*O*-*t*-butyl moiety and the rest of the molecule) were used as input to the *SHADE3* program to obtain better estimations of the $U_{\text{ani}}(\text{H})$ displacement parameters. The use of a transferred multipolar atom model allowed the reduction of $R(F)$ to 4.6% and $wR_2(F^2)$ to 7.2%, compared to 6.1% and 11.8%, respectively, for the neutral-spherical atom model, as refined in *MoPro*. The r.m.s. residual electron density was likewise reduced from 0.042 to 0.034 e \AA^{-3} .

Funding information

The authors are grateful to Ministère de l'Enseignement Supérieur et de la Recherche Scientifique de la République Islamique de Mauritanie and the Service de Coopération et

Table 4

Experimental details.

Crystal data	
Chemical formula	C ₇ H ₁₃ NO ₃
M_r	159.18
Crystal system, space group	Monoclinic, $P2_1/n$
Temperature (K)	293
a, b, c (Å)	6.0404 (6), 8.6114 (7), 17.6110 (17)
β (°)	98.771 (9)
V (Å ³)	905.35 (15)
Z	4
Radiation type	Mo $K\alpha$
μ (mm ⁻¹)	0.09
Crystal size (mm)	0.15 \times 0.1 \times 0.08
Data collection	
Diffraction	Bruker Kappa CCD
Absorption correction	–
No. of measured, independent and observed [$I > 2\sigma(I)$] reflections	2405, 2059, 1627
R_{int}	0.035
$(\sin \theta/\lambda)_{\text{max}}$ (Å ⁻¹)	0.650
Refinement	
$R[F^2 > 2\sigma(F^2)], wR(F^2), S$	0.034, 0.072, 1.00
No. of reflections	2059
No. of parameters	139
No. of restraints	31
H-atom treatment	Only H-atom coordinates refined
$\Delta\rho_{\text{max}}, \Delta\rho_{\text{min}}$ (e \AA^{-3})	0.16, –0.17

Computer programs: *APEX3* and *SAINT* (Bruker, 2016), *SHELXS97* (Sheldrick, 2008) and *MoPro* (Jelsch *et al.*, 2005).

d'Action Culturelle (SCAC) de l'Ambassade de France en Mauritanie for financial support.

References

- Allen, F. H. & Bruno, I. J. (2010). *Acta Cryst.* **B66**, 380–386.
- Brodesser, S., Mikeska, T., Nieger, M. & Kolter, T. (2003). *Acta Cryst.* **E59**, o1359–o1361.
- Bruker (2016). *APEX3* and *SAINT*. Bruker AXS Inc., Madison, Wisconsin, USA.
- Bruno, I. J., Cole, J. C., Edgington, P. R., Kessler, M., Macrae, C. F., McCabe, P., Pearson, J. & Taylor, R. (2002). *Acta Cryst.* **B58**, 389–397.
- Dibenedetto, A., Aresta, M., Fragale, C. & Narracci, M. (2002). *Green Chem.* **4**, 439–443.
- Domagała, S., Fournier, B., Liebschner, D., Guillot, B. & Jelsch, C. (2012). *Acta Cryst.* **A68**, 337–351.
- Ghosh, A. K. & Brindisi, M. (2015). *J. Med. Chem.* **58**, 2895–2940.
- Groom, C. R., Bruno, I. J., Lightfoot, M. P. & Ward, S. C. (2016). *Acta Cryst.* **B72**, 171–179.
- Jelsch, C., Ejsmont, K. & Huder, L. (2014). *IUCrJ*, **1**, 119–128.
- Jelsch, C., Guillot, B., Lagoutte, A. & Lecomte, C. (2005). *J. Appl. Cryst.* **38**, 38–54.
- Lee, H. K., Ten, L. N. & Pak, C. S. (1998). *Bull. Korean Chem. Soc.* **19**, 1148–1149.
- Madsen, A. Ø. & Hoser, A. A. (2014). *J. Appl. Cryst.* **47**, 2100–2104.
- Sebti, S., Rhihil, A. & Saber, A. (1996). *Chem. Lett.* **25**, 721.
- Sebti, S., Saber, A. & Rhihil, A. (1994). *Tetrahedron Lett.* **35**, 9399–9400.
- Sheldrick, G. M. (2008). *Acta Cryst.* **A64**, 112–122.
- Spackman, P. R., Turner, M. J., McKinnon, J. J., Wolff, S. K., Grimwood, D. J., Jayatilaka, D. & Spackman, M. A. (2021). *J. Appl. Cryst.* **54**, 1006–1011.

supporting information

Acta Cryst. (2022). E78, 1072-1076 [https://doi.org/10.1107/S2056989022009483]

Synthesis, crystal structure and Hirshfeld surface analysis of *tert*-butyl *N*-acetylcarbamate

Aly Dawa El Mestehdi, Moctar Abba, Mohamed Lemine El Housseine, Abderrahmane Ould Hadou, Aliou Hamady Barry, Brahim Ould Elemine, Christian Jelsch and Mohamed Gaye

Computing details

Data collection: *APEX3* (Bruker, 2016); cell refinement: *SAINTE* (Bruker, 2016); data reduction: *SAINTE* (Bruker, 2016); program(s) used to solve structure: *SHELXS97* (Sheldrick, 2008); program(s) used to refine structure: *MoPro* (Jelsch *et al.*, 2005); molecular graphics: *MoPro* (Jelsch *et al.*, 2005); software used to prepare material for publication: *MoPro* (Jelsch *et al.*, 2005).

tert-Butyl *N*-acetylcarbamate

Crystal data

$C_7H_{13}NO_3$

$M_r = 159.18$

Monoclinic, $P2_1/n$

Hall symbol: -P 2yn

$a = 6.0404$ (6) Å

$b = 8.6114$ (7) Å

$c = 17.6110$ (17) Å

$\beta = 98.771$ (9)°

$V = 905.35$ (15) Å³

$Z = 4$

$F(000) = 344$

$D_x = 1.168$ Mg m⁻³

Mo $K\alpha$ radiation, $\lambda = 0.71073$ Å

Cell parameters from 4200 reflections

$\theta = 2.4$ – 28.6 °

$\mu = 0.09$ mm⁻¹

$T = 293$ K

Block, colorless

$0.15 \times 0.1 \times 0.08$ mm

Data collection

Bruker Kappa CCD

diffractometer

Radiation source: fine-focus sealed tube

Graphite monochromator

CCD scans

2405 measured reflections

2059 independent reflections

1627 reflections with $I > 2\sigma(I)$

$R_{int} = 0.035$

$\theta_{max} = 27.5$ °, $\theta_{min} = 2.6$ °

$h = -7 \rightarrow 7$

$k = 0 \rightarrow 11$

$l = 0 \rightarrow 22$

Refinement

Refinement on F^2

Least-squares matrix: full

$R[F^2 > 2\sigma(F^2)] = 0.034$

$wR(F^2) = 0.072$

$S = 1.00$

2059 reflections

139 parameters

31 restraints

Primary atom site location: structure-invariant direct methods

Secondary atom site location: difference Fourier map

Hydrogen site location: difference Fourier map

Only H-atom coordinates refined

$w = 1/[4.4\sigma^2(F_o^2)]$

$(\Delta/\sigma)_{max} = 0.002$

$$\Delta\rho_{\max} = 0.16 \text{ e } \text{\AA}^{-3}$$

$$\Delta\rho_{\min} = -0.17 \text{ e } \text{\AA}^{-3}$$

Extinction correction: Isotropic Gaussian
 Extinction coefficient: 0.51132

Special details

Refinement. Refinement of F^2 against reflections. The threshold expression of $F^2 > 2\sigma(F^2)$ is used for calculating R-factors(gt) and is not relevant to the choice of reflections for refinement. R-factors based on F^2 are statistically about twice as large as those based on F , and R-factors based on ALL data will be even larger.

Fractional atomic coordinates and isotropic or equivalent isotropic displacement parameters (\AA^2)

	<i>x</i>	<i>y</i>	<i>z</i>	$U_{\text{iso}}^*/U_{\text{eq}}$
O1	0.38211 (11)	0.355396 (15)	0.40123 (4)	0.05484 (14)
O2	0.63464 (12)	0.29985 (8)	0.32233 (4)	0.06801 (17)
O3	0.73388 (12)	-0.08048 (8)	0.46784 (4)	0.06574 (16)
N1	0.57479 (13)	0.14069 (8)	0.42246 (5)	0.05046 (16)
H1	0.474 (2)	0.1271 (16)	0.4629 (7)	0.08754
C5	0.54053 (15)	0.27070 (10)	0.37571 (5)	0.04754 (17)
C6	0.73373 (15)	0.02549 (11)	0.42216 (6)	0.05121 (18)
C1	0.30097 (15)	0.50254 (10)	0.36327 (6)	0.05446 (18)
C7	0.89889 (19)	0.03248 (14)	0.36770 (7)	0.0716 (3)
H7A	1.0210 (16)	-0.0607 (14)	0.3829 (8)	0.10454
H7B	0.9899 (18)	0.1427 (14)	0.3755 (9)	0.11089
H7C	0.818 (2)	0.0353 (17)	0.3076 (6)	0.11503
C4	0.18467 (19)	0.46831 (14)	0.28329 (7)	0.0740 (3)
H4A	0.3039 (17)	0.4270 (16)	0.2468 (6)	0.10880
H4B	0.106 (2)	0.5761 (14)	0.2597 (8)	0.11611
H4C	0.0505 (16)	0.3836 (15)	0.2852 (8)	0.11411
C3	0.4904 (2)	0.61607 (13)	0.36559 (8)	0.0758 (2)
H3A	0.578 (2)	0.6274 (16)	0.4245 (8)	0.11708
H3B	0.419 (2)	0.7310 (12)	0.3505 (9)	0.12094
H3C	0.6142 (17)	0.5881 (15)	0.3283 (7)	0.10779
C2	0.1345 (2)	0.55587 (15)	0.41419 (8)	0.0822 (3)
H2A	0.0073 (16)	0.4648 (14)	0.4127 (9)	0.11714
H2B	0.054 (2)	0.6620 (14)	0.3891 (8)	0.12347
H2C	0.232 (2)	0.5828 (17)	0.4703 (7)	0.12492

Atomic displacement parameters (\AA^2)

	U^{11}	U^{22}	U^{33}	U^{12}	U^{13}	U^{23}
O1	0.0660 (4)	0.0489 (4)	0.0515 (4)	0.0085 (3)	0.0150 (3)	0.0127 (3)
O2	0.0786 (5)	0.0669 (5)	0.0644 (5)	0.0061 (4)	0.0300 (4)	0.0184 (3)
O3	0.0745 (5)	0.0484 (4)	0.0771 (5)	0.0077 (3)	0.0204 (4)	0.0162 (3)
N1	0.0599 (5)	0.0439 (4)	0.0495 (5)	0.0021 (3)	0.0144 (3)	0.0091 (3)
H1	0.09872	0.08344	0.09180	0.02741	0.05087	0.03885
C5	0.0539 (5)	0.0441 (5)	0.0456 (5)	-0.0003 (4)	0.0107 (4)	0.0056 (4)
C6	0.0573 (5)	0.0430 (5)	0.0533 (5)	-0.0001 (4)	0.0083 (4)	0.0024 (4)
C1	0.0592 (5)	0.0460 (5)	0.0551 (5)	0.0050 (4)	-0.0011 (4)	0.0103 (4)
C7	0.0720 (7)	0.0747 (7)	0.0731 (7)	0.0168 (6)	0.0274 (6)	0.0133 (6)
H7A	0.09887	0.10412	0.11797	0.04100	0.04001	0.02395

H7B	0.08822	0.09468	0.16018	-0.00028	0.05229	0.03275
H7C	0.14423	0.13621	0.06953	0.04903	0.03193	0.00590
C4	0.0757 (7)	0.0794 (8)	0.0597 (7)	-0.0079 (6)	-0.0129 (5)	0.0126 (6)
H4A	0.12776	0.13382	0.06263	0.00285	0.00747	0.00354
H4B	0.11933	0.11272	0.10174	0.01287	-0.02973	0.03707
H4C	0.09893	0.11674	0.11538	-0.03490	-0.01984	0.00269
C3	0.0723 (7)	0.0514 (6)	0.0968 (9)	-0.0083 (5)	-0.0096 (6)	0.0110 (6)
H3A	0.11467	0.09511	0.12396	-0.01659	-0.03780	-0.00724
H3B	0.11702	0.05611	0.17940	-0.00332	-0.01031	0.02819
H3C	0.08755	0.09430	0.14362	-0.01523	0.02433	0.02842
C2	0.0844 (8)	0.0751 (8)	0.0889 (9)	0.0249 (6)	0.0193 (6)	0.0046 (7)
H2A	0.09735	0.11323	0.15160	0.01562	0.05342	0.02003
H2B	0.12561	0.09416	0.15181	0.05340	0.02495	0.01964
H2C	0.15392	0.13217	0.08898	0.04922	0.01950	-0.01800

Geometric parameters (Å, °)

O1—C5	1.3344 (11)	C7—H7A	1.0950
O1—C1	1.4808 (9)	C7—H7B	1.0950
O2—C5	1.1970 (11)	C4—H4C	1.0950
O3—C6	1.2164 (11)	C4—H4A	1.0950
N1—C5	1.3864 (12)	C4—H4B	1.0950
N1—C6	1.3811 (12)	C3—H3C	1.0950
N1—H1	1.013 (8)	C3—H3B	1.0950
C6—C7	1.4868 (15)	C3—H3A	1.0950
C1—C3	1.5009 (14)	C2—H2C	1.0950
C1—C4	1.5042 (15)	C2—H2B	1.0950
C1—C2	1.5170 (16)	C2—H2A	1.0950
C7—H7C	1.0950		
C5—O1—C1	121.38 (6)	H7C—C7—H7B	104 (1)
C5—N1—C6	128.22 (7)	H7A—C7—H7B	107.3 (8)
C5—N1—H1	117.3 (7)	C1—C4—H4C	110.1 (7)
C6—N1—H1	114.4 (7)	C1—C4—H4A	111.0 (6)
O1—C5—O2	126.91 (8)	C1—C4—H4B	107.6 (6)
O1—C5—N1	106.93 (7)	H4C—C4—H4A	111 (1)
O2—C5—N1	126.15 (7)	H4C—C4—H4B	107.3 (10)
O3—C6—N1	117.82 (7)	H4A—C4—H4B	110 (1)
O3—C6—C7	121.61 (8)	C1—C3—H3C	115.4 (7)
N1—C6—C7	120.57 (8)	C1—C3—H3B	108.2 (6)
O1—C1—C3	110.28 (7)	C1—C3—H3A	109.8 (7)
O1—C1—C4	109.28 (7)	H3C—C3—H3B	109 (1)
O1—C1—C2	101.29 (7)	H3C—C3—H3A	108.3 (10)
C3—C1—C4	113.48 (8)	H3B—C3—H3A	105 (1)
C3—C1—C2	110.99 (9)	C1—C2—H2C	106.5 (7)
C4—C1—C2	110.85 (9)	C1—C2—H2B	107.8 (8)
C6—C7—H7C	112.4 (7)	C1—C2—H2A	107.1 (7)
C6—C7—H7A	107.8 (6)	H2C—C2—H2B	109.3 (10)

C6—C7—H7B	109.1 (7)	H2C—C2—H2A	117 (1)
H7C—C7—H7A	115.8 (9)	H2B—C2—H2A	108.8 (10)
O1—C5—N1—C6	-174.66 (12)	H1—N1—C6—C7	-178 (1)
O1—C5—N1—H1	4 (1)	C5—O1—C1—C3	-60.18 (11)
O1—C1—C3—H3C	71.1 (8)	C5—O1—C1—C4	65.21 (11)
O1—C1—C3—H3B	-166.1 (9)	C5—O1—C1—C2	-177.77 (12)
O1—C1—C3—H3A	-51.6 (9)	C5—N1—C6—C7	1.01 (14)
O1—C1—C4—H4C	55.5 (7)	C4—C1—C3—H3C	-51.9 (7)
O1—C1—C4—H4A	-67.8 (7)	C4—C1—C3—H3B	70.9 (7)
O1—C1—C4—H4B	172.1 (9)	C4—C1—C3—H3A	-174.6 (9)
O1—C1—C2—H2C	66.4 (7)	C4—C1—C2—H2C	-177.8 (9)
O1—C1—C2—H2B	-176.4 (7)	C4—C1—C2—H2B	-60.5 (7)
O1—C1—C2—H2A	-59.4 (7)	C4—C1—C2—H2A	56.4 (8)
O2—C5—O1—C1	0.45 (12)	H4A—C4—C1—C3	56 (1)
O2—C5—N1—C6	5.90 (14)	H4A—C4—C1—C2	-179 (1)
O2—C5—N1—H1	-175 (1)	H4B—C4—C1—C3	-64 (1)
O3—C6—N1—C5	-179.23 (13)	H4B—C4—C1—C2	61 (1)
O3—C6—N1—H1	2 (1)	H4C—C4—C1—C3	179 (1)
O3—C6—C7—H7C	121.4 (9)	H4C—C4—C1—C2	-55 (1)
O3—C6—C7—H7A	-7.4 (8)	C3—C1—C2—H2C	-50.7 (7)
O3—C6—C7—H7B	-123.6 (8)	C3—C1—C2—H2B	66.5 (8)
N1—C5—O1—C1	-178.99 (12)	C3—C1—C2—H2A	-176.5 (8)
N1—C6—C7—H7C	-58.8 (8)	H3A—C3—C1—C2	60 (1)
N1—C6—C7—H7A	172.4 (8)	H3B—C3—C1—C2	-55 (1)
N1—C6—C7—H7B	56.1 (8)	H3C—C3—C1—C2	-177 (1)

Hydrogen-bond geometry (Å, °)

<i>D</i> —H \cdots <i>A</i>	<i>D</i> —H	H \cdots <i>A</i>	<i>D</i> \cdots <i>A</i>	<i>D</i> —H \cdots <i>A</i>
C4—H4A \cdots O2	1.10	2.48	3.0651 (14)	112
C3—H3C \cdots O2	1.10	2.49	2.9928 (15)	107
N1—H1 \cdots O3 ⁱ	1.01 (1)	1.92 (1)	2.9285 (11)	173 (1)

Symmetry code: (i) $-x+1, -y, -z+1$.